STEM CELLS AND DEVELOPMENT
Volume 23, Number 13, 2014

DOI: 10.1089/scd.2013.0600

let-7 Enhances Osteogenesis and Bone Formation While Repressing Adipogenesis of Human Stromal/Mesenchymal Stem Cells by Regulating HMGA2

Jianfeng Wei,[1] Hongling Li,[1] Shihua Wang,[1] Tangping Li,[1] Junfen Fan,[1] Xiaolei Liang,[1] Jing Li,[1] Qin Han,[1] Li Zhu,[1] Linyuan Fan,[1] and Robert Chunhua Zhao[1,2]

Bone and fat cells share a common progenitor, stromal/mesenchymal stem cells (MSCs), that can differentiate into osteoblasts or adipocytes. Osteogenesis and adipogenesis of MSCs maintain homeostasis under physiological conditions. The disruption of this homeostasis leads to bone-related metabolic diseases. For instance, reduction in bone formation, which is usually accompanied by an increase in bone marrow adipogenesis, occurs with aging, immobility, or osteoporosis. Thus, it is crucial to gain an understanding of how osteogenic and adipogenic lineages of MSCs are regulated. Here, we present evidence that *let-7* is a positive regulator of bone development. Using gain- and loss-of-function approaches, we demonstrate that *let-7* markedly promotes osteogenesis and suppresses adipogenesis of MSCs in vitro. Moreover, *let-7* could promote ectopic bone formation of MSCs in vivo. Subsequent studies further demonstrated that *let-7*'s effects are mediated through the repression of high-mobility group AT-hook 2 (HMGA2) expression. RNAi depletion of HMGA2 could also enhance osteogenesis and repress adipogenesis. Overall, we found a novel role of *let-7*/HMGA2 axis in regulating the balance of osteogenesis and adipogenesis of MSCs. Thus, *let-7* can be used as a novel therapeutic target for disorders that are associated with bone loss and adipocyte accumulation.

Introduction

Human mesenchymal/stromal stem cells (hMSCs) have the capacity of multilineage differentiation into cells comprising bone, cartilage, adipose, and muscle [1–4]. Osteogenesis and adipogenesis of MSCs maintain homeostasis under physiological conditions. With aging, menopause, or ovariectomy, the balance between adipogenic and osteogenic differentiation of MSCs can be disrupted, leading to excessive accumulation of bone marrow adipocytes and a decrease in bone mass (eg, osteoporosis) [5]. Therefore, clarifying the balance of factors that control bone formation and adipogenesis of MSCs might lead to novel approaches for the prevention and treatment of disorders related to osteogenesis and adipogenesis.

MicroRNAs (miRNAs) are a class of small, non-coding RNA molecules that function as negative regulators of gene expression at the post-transcriptional level [6,7]. Emerging evidence suggests that miRNAs are involved in regulating differentiation and cell fate decisions [8]. Lots of miRNAs, including miR-143, miR-24, miR-31, miR-30c, miR-642a-3p, miR-141/200a, miR-135, miR-378, miR-196a, miR-27a, miR-26a, miR-125b, miR-133, miR-29b, miR-2861, miR-3960, miR-335-5p, miR-138, and miR-130, have been identified that are involved in the differentiation of adipocytes or osteoblasts [9–22]. Recently, several miRNAs have also been identified to be responsible for the balance of adipogenesis and osteogenesis. Overexpression of miR-204, miR-17-5p, and miR-106a suppresses osteoblast differentiation and promotes adipocyte differentiation [23,24]. In contrast, miR-637 has an opposite effect, suggesting that adipocyte and osteoblast differentiation are tightly regulated by specific miRNAs in hMSCs [25]. As the first known human family of miRNAs, the *let-7* family has 10 mature members that are produced from 13 precursor sequences [26]. *let-7* miRNA family controls many cell-fate determination genes and influences pluripotency, differentiation, tumorigenesis, and transformation [26–29]. Recently, the role of *let-7* in modulating adipocyte differentiation by the direct targeting of high-mobility group AT-hook 2 (HMGA2) was discovered [19]. In addition, inhibition of the platelet-derived growth factor pathway during osteogenic differentiation of MSCs resulted in reduced expression of several miRNAs, including *let-7* [30]. However, the precise functions of *let-7*

[1]Institute of Basic Medical Sciences Chinese Academy of Medical Sciences, Center of Excellence in Tissue Engineering, School of Basic Medicine Peking Union Medical College, Beijing, China.
[2]Peking Union Medical College Hospital, Beijing, China.

in osteogenesis and the underlying molecular mechanisms remain largely unknown. HMGA2 has been found to be a well-established target gene of *let-7* [31,32], but how *let-7*/HMGA2 axis regulates osteogenesis is not known until now.

In the present study, we detected the dynamic miRNA expression pattern in femurs of mice (embryos from 15–21 days of gestation to 1- to 6-week-old males) and found that *let-7* is a positive regulator of bone development. Gain- and loss-of-function analysis showed that *let-7* can promote osteogenic differentiation, suppress adipogenesis of human adipose-derived mesenchymal stem cells (hADSCs) in vitro, and enhance bone formation in vivo as shown by the detection of expression of Runt-related transcription factor 2 (Runx2), bone sialoprotein (BSP), osteocalcin (OC), and type I collagen alpha 1 (Col1α1) (late marker of osteogenesis) as well as alkaline phosphatase (ALP) and osteopontin (OPN) (early marker of osteogenesis). Our findings indicated that *let-7* was involved in the lineage specification of hADSCs through the targeting of HMGA2. Inhibition of HMGA2 could mimic the effect of *let-7* overexpression on osteogenesis and adipogenesis. This evidence prompted us to conclude that *let-7* may serve as a novel therapeutic target for osteogenesis- or adipogenesis-related disorders.

Materials and Methods

Isolation and culture of hADSCs

The hADSCs were isolated from human adipose tissues that were obtained from donors undergoing tumescent liposuction according to the procedure approved by the Ethics Committee at the Chinese Academy of Medical Sciences and the Peking Union Medical College. The isolation and culture procedure of hADSCs was adapted from our previous article [33]. hADSCs in the third passage were used for the following experiments. Adipogenic and osteogenic differentiation of hADSCs was performed as described earlier [23,24]. hADSCs from three different individuals were used as biological replicates.

ALP staining, alizarin red staining, and oil red O staining

ALP staining was typically performed using the ALP staining kit (Institute of Hematology and Blood Diseases Hospital, Chinese Academy of Medical Sciences) according to the manufacturer's instructions. Alizarin red and oil red O staining were performed according to previous articles [23,24].

ALP activity assay

ALP activity assay was performed using the Alkaline Phosphatase Yellow (pNPP) Liquid Substrate System for ELISA. ALP activity was calculated according to the manufacturer's instructions (ALP diagnostics kit; Sigma-Aldrich). ALP activity was normalized to the total protein of cell lysates.

Masson's trichrome staining

Masson's trichrome staining was performed according to standard procedures using the Trichrome Stain (Masson) kit (Sigma-Aldrich).

Lentiviral vector preparation and infection

Lentivirus production was carried out according to protocols from GenePharma (www.genepharma.com/). After cells were infected with *let-7* overexpression lentiviral vector, GFP-positive cells were sorted by an FACSCalibur (BD) Flow Cytometer.

miRNA inhibitor, and siRNA transfection

Cells were transfected with single-stranded oligonucleotides corresponding to the mature miRNA sequence as an inhibitor pool of *let-7* family miRNAs by Lipofectamine 2000 (Invitrogen) according to the manufacturer's instructions. All oligonucleotides were obtained from GenePharma. The siRNA targeting HMGA2 was synthesized (Invitrogen). The siRNA was transfected into cells with the procedure used for miRNA transfection. The sequences of miRNA inhibitor of let-7 family and siRNA targeting HMGA2 are listed in Supplementary Tables S1 and S2.

Dual luciferase reporter genes constructs and assays

let-7 recognition sites of the target genes were cloned in the 3′-untranslated region (3′-UTR) containing the predicted seed match site or the mutant (mu) site of the firefly luciferase reporter vector according to standard protocols. Eighty to100 bp synthetic fragments were cloned in between the *Xho*I and *Not*I cleavage sites of the pRL-TK vector (Promega). The oligonucleotide sequences are shown in Figure 5. A total of 5×10^4 293T cells were co-transfected with 1 μg pRL-TK vector with or without the synthetic fragment of the predicted target genes 3′-UTR, pGL-3 vector with luciferase reporter gene, and 100 nM *let-7* mimics or miR-NC mixed with lipofectamine 2000 (Invitrogen), respectively, according to the manufacturer's instructions. Lysates were harvested at 24 h after transfection. Luciferase activity was measured in triplicate by using the Dual Luciferase Reporter Assay System (Promega). Firefly luciferase activity was normalized to Renilla luciferase activity.

RNA isolation and qRT-PCR analysis

Total RNA was extracted from cultured cells or fresh bone tissues with TRIzol reagent (Invitrogen). The mRNA levels were assayed with the primer sets in the Fast Real-Time PCR system (Applied Biosystems). The miRNA was extracted with the miRVana Isolation kit (Ambion) as described by the manufacturer. The miRNA levels were assayed according to the manufacturer's instructions by TaqMan Small RNA assays (Invitrogen). Relative expression of mRNA or miRNA was evaluated by the $2^{-\Delta\Delta Ct}$ method and normalized to GAPDH or U6, respectively. Primers of mRNA real-time PCR are listed in Table 1.

Western blot

Protein was extracted with radioimmunoprecipitation lysis buffer with PMSF (Beyotime) and quantified with BCA Protein Assay kit (Beyotime). Lysates were electrophoresed on 10% sodium dodecyl sulfate–polyacrylamide gel electrophoresis and transferred to polyvinylidene difluoride

Table 1. Real-Time PCR Primers Sequence Used in This Study

Gene	*Forward primer (5′-3′)*	*Reverse primer (5′-3′)*
RUNX2	TGTCATGGCGGGTAACGAT	AAGACGGTTATGGTCAAGGTGAA
ALP	CCACGTCTTCACATTTGGTG	AGACTGCGCCTGGTAGTTGT
OC	GGCGCTACCTGTATCAATGG	GTGGTCAGCCAACTCGTCA
OPN	ACTCGAACGACTCTGATGATGT	GTCAGGTCTGCGAAACTTCTTA
GAPDH	GGTCACCAGGGCTGCTTTTA	GGATCTCGCTCCTGGAAGATG

membrane. The blots were probed with primary antibodies at 4°C overnight and then probed with horseradish peroxidase-conjugated secondary antibodies (1:2,000; Zsbio). Antibody–antigen complexes were detected using an ECL reagent (Millipore).

In vivo bone formation assay

All procedures involving mice were performed in accordance with institutional guidelines and permissions of the Ethics Committee at the Chinese Academy of Medical Sciences and the Peking Union Medical College. Approximately 5×10^5 hADSCs infected with Lenti-*let-7c* and Lenti-scr were loaded in PLGA scaffolds and implanted into 6-week-old male athymic mice (BALB/c nu/nu strain) (12 mice/group) for 60 days. The xenografts were removed for subsequent experiments.

Immunofluorescence staining

Cells were fixed with 4% formaldehyde (Sigma-Aldrich) in phosphate-buffered saline (PBS) for 30 min at room temperature, permeabilized with 0.1% Triton X-100 in PBS for 15 min, and then blocked with 3% bovine serum albumin (BSA; Sigma-Aldrich) in PBS for 30 min. Thereafter, cells were incubated with primary antibody at 4°C overnight, incubated in the specified secondary antibodies for 1 h, and visualized with an Olympus IX71 fluorescence microscope that was equipped with an Olympus DP72 imaging system.

Immunohistochemical analysis

After xenograft implantation for 60 days, the mice were killed, and their tissues were fixed overnight, processed, sectioned according to standard procedures, and stained with hematoxylin and eosin (H&E). The sections were permeabilized with 0.1% Triton X-100 in PBS for 15 min, blocked with 3% BSA (Sigma-Aldrich) in PBS for 30 min, and thereafter incubated with primary antibody at 4°C overnight. Next, sections were processed using the ABC detection kit (Vector Laboratories). Sections were visualized with an Olympus BX51 light microscope that was equipped with an Olympus DP70 camera.

Statistical analysis

The data are presented as the mean ± SD. Student's *t*-test, and one-way ANOVA was used to test the differences between groups. The results were considered significant if $P < 0.05$. Calculations were performed with SPSS software version 19.0.

Results

The expression pattern of let-7 suggests that it might be a candidate enhancer in bone formation and osteogenesis

In our study, we detected the dynamic expression pattern of *let-7c* and *let-7d* in the mouse femur (embryos from 15–21 days of gestation to 1- to 6-week-old male C57BL/6J mice) by TaqMan qRT-PCR. The results showed that *let-7c* and *let-7d* were expressed at relatively low levels in embryos and markedly increased after birth. Expression peaked in 4-week-old mice and rapidly decreased thereafter (Fig. 1A, B). Previous reports demonstrated that bone formation and mineral apposition rates decrease rapidly from the fourth week onward in male C57BL/6J mice [34]. We confirmed that the peak in the expression of *let-7c* and *let-7d* was consistent with the bone development phase. To confirm the expression profile of *let-7* in osteogenesis in vitro, the expression patterns of *let-7c* and *let-7d* were analyzed on day 0, 2, 4, and 6 of osteogenic differentiation using TaqMan qRT-PCR (Fig. 1C, D). Results showed that the expression level of *let-7* was up-regulated when hADSCs underwent differentiation toward osteogenic lineages.

Up-regulation of let-7 promotes osteogenic differentiation and suppresses adipogenesis of hADSCs

An initial small-scale screen using miRNA mimics showed that all *let-7* family members could actually promote osteogenic differentiation and repress adipogenesis in hADSCs, suggesting that this large family of miRNAs is functionally similar. This is consistent with previous observations that *let-7* and its family members are highly conserved across species in sequence and function [26]. Furthermore, the dynamic miRNA expression pattern of *let-7c* and *d* orthologs is similar in femurs of mice and hADSCs; therefore, we chose to focus on *let-7c*.

The expression of *let-7c* was up-regulated by expressing its precursor in hADSCs with a lentiviral vector (Lenti-*let-7c*). The same lentiviral vector expressing a scrambled sequence (Lenti-scr) with no homology to the human genome was used as a parallel control. TaqMan qRT-PCR confirmed that the expression of *let-7c* was up-regulated by more than 400-fold in Lenti-*let-7c*-infected hADSCs (data not shown). Lenti-*let-7c*-infected hADSCs were induced to differentiate to the osteoblast lineage with standard osteogenic induction media. ALP staining and activity assays

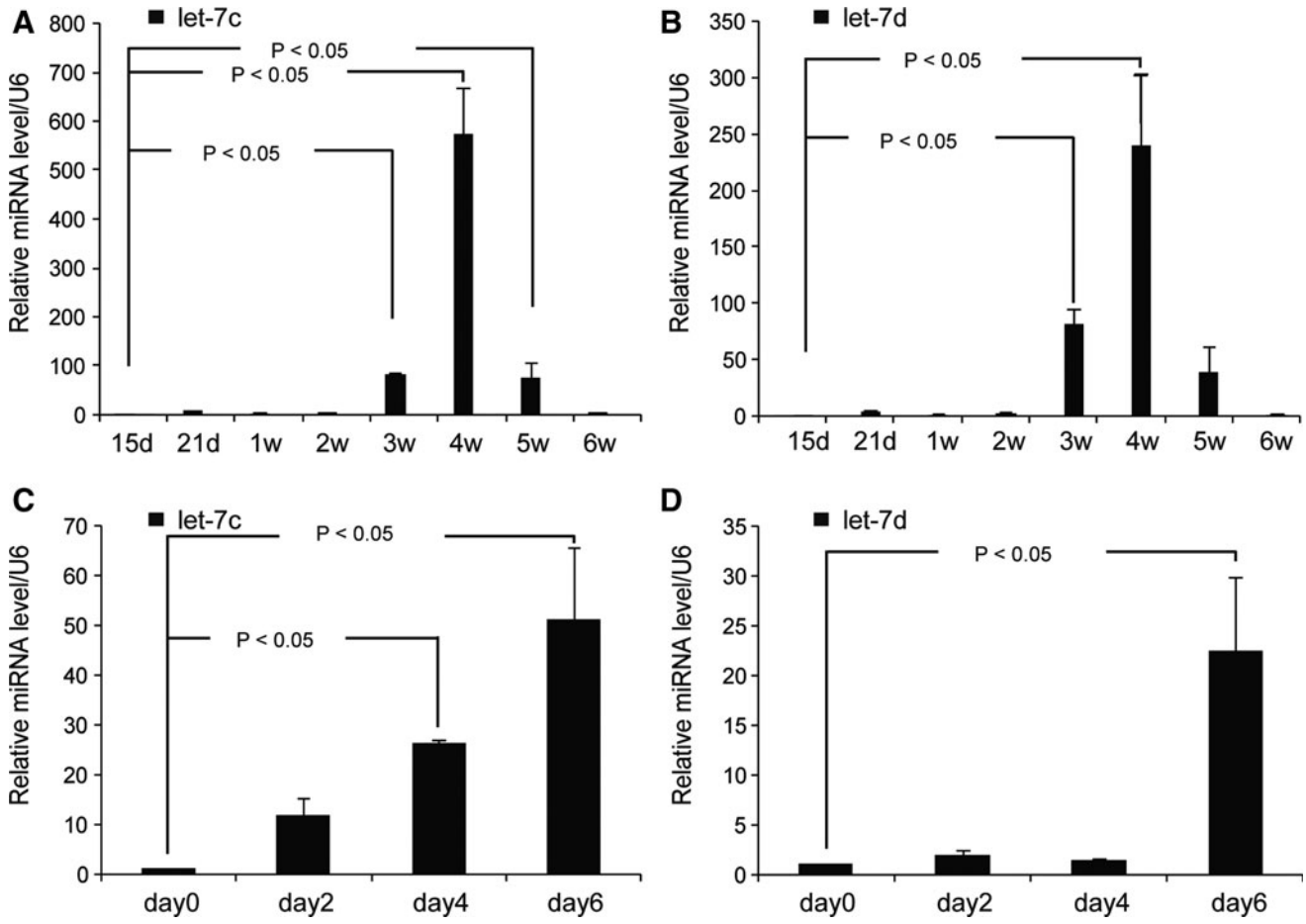

FIG. 1. *let-7* expression profiles during bone formation and osteogenesis differentiation. **(A, B)** The expression of *let-7c* and *let-7d*, respectively, in different developmental stages of the mouse femur was detected using TaqMan qRT-PCR. U6 was used as an internal normalization control. The data are presented as the mean ± SD from three independent trials. **(C, D)** TaqMan qRT-PCR analysis of the dynamic expression pattern of *let-7c* was performed in human adipose-derived mesenchymal stem cells (hADSCs) at days 0, 2, 4, and 6 of osteogenic differentiation. U6 was used as an internal normalization control. The data are presented as the mean ± SD from three independent trials.

confirmed that the expression and activity of ALP, an early marker of osteoblasts, were increased by *let-7c* overexpression (Fig. 2A–C). Alizarin red staining indicated that matrix mineralization was enhanced in *let-7c*-upregulated cells (Fig. 2D).

Immunofluorescence staining and western blot analysis indicated that the protein levels of ALP, OPN, and Runx2 were upregulated in Lenti-*let-7c*-infected hADSCs (Fig. 2E–G). As shown by qRT-PCR, Runx2, ALP, and OPN were increased in *let-7*-overexpressed hADSCs during osteogenesis

FIG. 2. Overexpression of *let-7* promotes osteogenic differentiation and suppresses adipogenesis of hADSCs; the expression of *let-7* was up-regulated by expressing the *let-7c* precursor with a lentiviral vector (Lenti-*let-7c*), and the same lentiviral vector expressing a scrambled sequence (Lenti-scr) was used as a parallel control. **(A)** Alkaline phosphatase (ALP) staining indicated the effect on osteogenic differentiation of Lenti-*let-7c*-infected hADSCs compared with Lenti-scr-infected cells at day 4. $n = 5$. Scale bars: 100 μm. **(B)** ALP-positive cells were counted under a high power field and normalized by the total cell numbers in infected cells. The data are presented as the mean ± SD from five independent images of each group. **(C)** ALP activity was analyzed in hADSCs infected with Lenti-*let-7c* and Lenti-scr during osteogenic differentiation at day 4. $n = 3$. **(D)** Alizarin red staining indicated the mineralization in hADSCs infected with Lenti-*let-7c* and Lenti-scr after induction to the osteogenic lineage at day 14. $n = 3$. Scale bars: 100 μm. **(E, F)** Immunofluorescence analysis of the expression of ALP and Runt-related transcription factor 2 (Runx2) with Hoechst 33342 counterstaining in hADSCs infected with Lenti-*let-7c* and Lenti-scr after induction to the osteogenic lineage at day 4. Scale bars: 100 μm. **(G)** The protein expression of ALP, osteopontin (OPN), and Runx2 was measured by western blot analysis in hADSCs infected with Lenti-*let-7c* and Lenti-scr after inducing osteogenic differentiation at day 4. $n = 3$. **(H)** The mRNA expression levels of Runx2, ALP, OPN, and osteocalcin (OC) were analyzed by qRT-PCR in hADSCs infected with Lenti-*let-7c* and Lenti-scr after induction to the osteogenic lineage at day 4. The data are presented as the mean ± SD from three independent trials. **(I)** Oil red O staining indicated the effect of *let-7* overexpression on adipogenic differentiation of hADSCs at day 12. $n = 4$. Scale bars: 100 μm. **(J)** The dye in cells was extracted with isopropanol, and the OD value was measured at a wavelength of 510 nm using a microplate reader for quantitation. The data are presented as the mean ± SD from five independent trials. Color images available online at www.liebertpub.com/scd

(Fig. 2H). To further elucidate the effect of *let-7* on the adipogenic differentiation of hADSCs, Lenti-*let-7c*-infected hADSCs were induced to differentiate to the adipogenic lineage. Overexpression of *let-7* inhibited adipogenesis as indicated by oil red O staining (Fig. 2I, J). This is consistent with a previous report that *let-7* inhibits adipogenesis in 3T3-L1 cells [19].

Down-regulation of endogenous let-7 suppresses osteogenic differentiation and enhances adipogenesis of hADSCs

To further study the effect of *let-7* on osteogenic differentiation, we used specific inhibitors to reduce endogenous expression of *let-7*. miRNA-specific qRT-PCR analysis

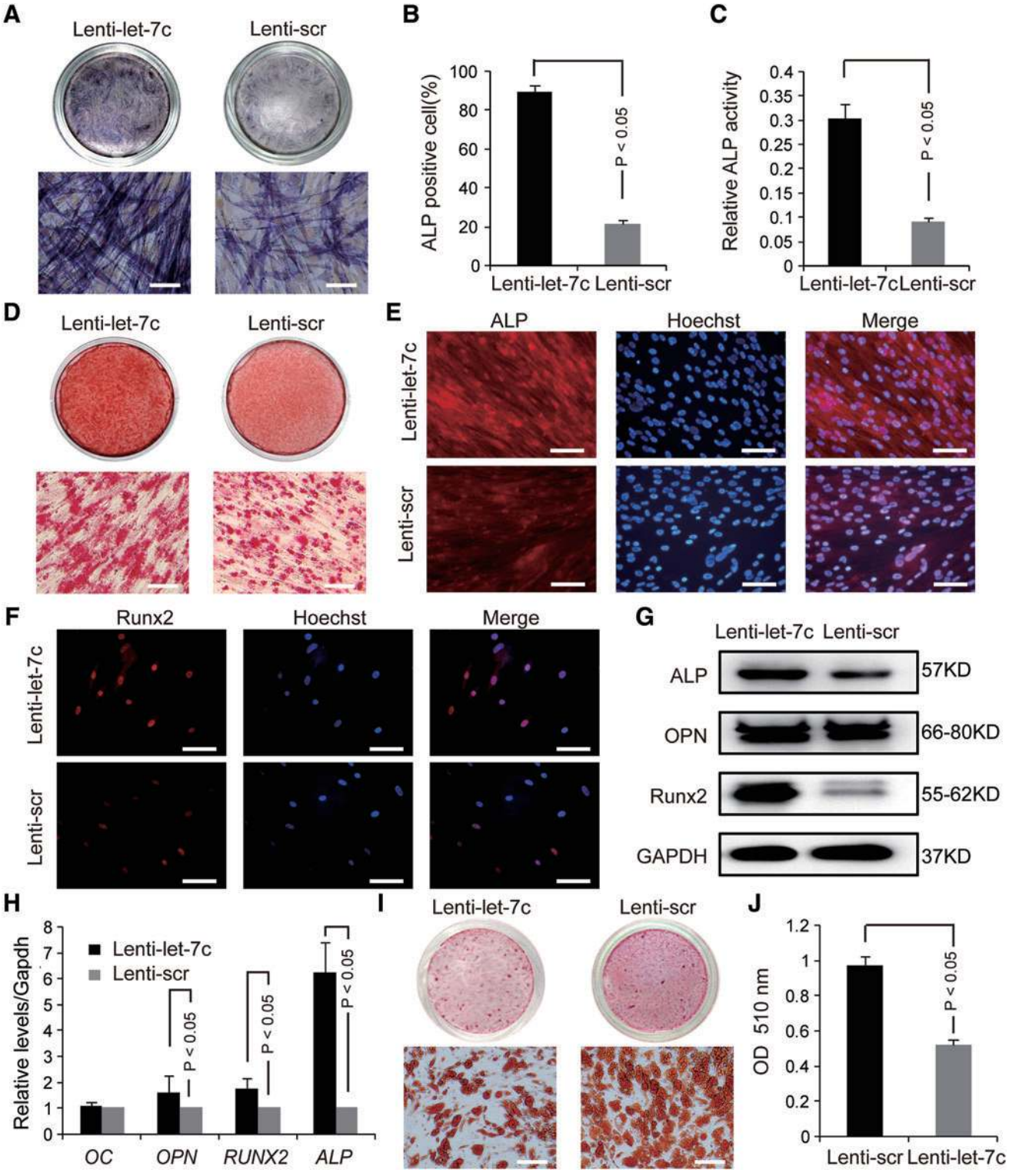

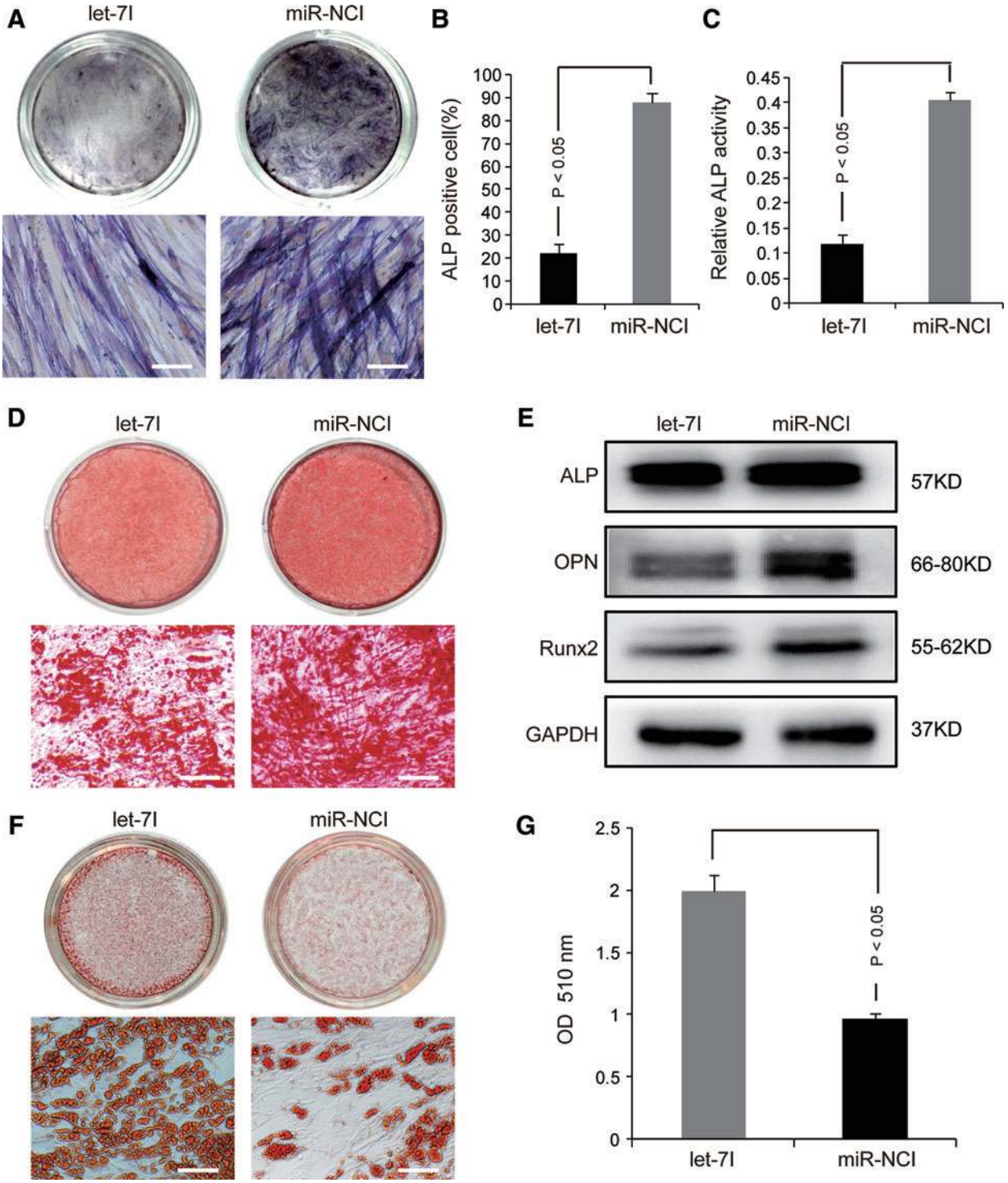

FIG. 3. Down-regulation of endogenous *let-7* suppresses osteogenic differentiation and promotes adipogenic differentiation of hADSCs; a specific inhibitor of *let-7* (*let-7*I) was transfected into hADSCs to inhibit its endogenous expression. **(A)** ALP staining indicated the effect of *let-7* down-regulation on osteogenic differentiation of hADSCs at day 6. $n=3$. Scale bars: 100 μm. **(B)** ALP-positive cells were counted under a high power field and normalized by the total cell number of hADSCs transfected with *let-7* inhibitor and negative control miRNA inhibitor (miR-NCI) after inducing osteogenic differentiation at day 6. The data are presented as the mean ± SD from five independent images of each group. **(C)** ALP activity was calculated in *let-7c*-down-regulated and negative control hADSCs after induction to the osteogenic lineage at day 6. $n=3$. **(D)** Alizarin red staining for mineralization indicated the effect of osteogenic differentiation of *let-7*-down-regulated and negative control hADSCs at day 14. $n=3$. Scale bars: 100 μm. **(E)** Western blot analysis evaluated the expression of ALP, OPN, and Runx2 in *let-7*-down-regulated and negative control hADSCs undergoing osteogenic differentiation at day 6. $n=3$. **(F)** Oil red O staining indicated the effect of *let-7* down-regulation on adipogenesis of hADSCs at day 12. $n=3$. Scale bars: 100 μm. **(G)** The dye of oil red O-positive cells was extracted by isopropanol, and the OD value was quantified at 510 nm wavelength. The data are presented as the mean ± SD from four independent trials. miR-NCI was used as a control. *let-7*I, *let-7* inhibitor. Color images available online at www.liebertpub.com/scd

showed that inhibitors effectively inhibited *let-7* expression compared with negative control inhibitors (Supplementary Fig. S1; Supplementary Data are available online at www.liebertpub.com/scd). Then, *let-7*-inhibited hADSCs were induced to differentiate to the osteogenic lineage. The results of ALP staining and ALP activity assays showed that the inhibition of endogenous *let-7* significantly decreased the osteogenic differentiation of hADSCs compared with cells transfected with a negative control miRNA inhibitor (miR-NCI) (Fig. 3A–C). Alizarin red staining showed that the matrix mineralization was also suppressed during osteogenic differentiation of *let-7*-inhibited hADSCs (Fig. 3D). These results confirmed that down-regulation of *let-7* can sharply decrease the osteogenic differentiation of hADSCs.

Consistent with these results, western blot analysis showed that the expression levels of Runx2, OPN, and ALP were decreased when *let-7* was inhibited during the osteogenesis of hADSCs (Fig. 3E). These results indicate that *let-7* is a positive regulator of osteogenesis in hADSCs. However, oil red O staining showed that the down-regulation of *let-7* significantly promoted the adipogenesis of hADSCs (Fig. 3F, G).

let-7 promotes ectopic bone formation of hADSCs in vivo

To clarify whether up-regulation of *let-7* can enhance ectopic bone formation in vivo, hADSCs infected with Lenti-*let-7c* and Lenti-scr were loaded in PLGA scaffolds and implanted into 6-week-old male athymic mice (BALB/c nu/nu strain) for 60 days (Fig. 4A, B). Significant differences between hADSC xenografts infected with Lenti-*let-7c* and those infected with Lenti-scr were observed by H&E staining and Masson's trichrome staining (Fig. 4C, D). Bone tissue and Blue collagen in hADSC xenografts overexpressing *let-7c* were more abundant than in the Lenti-scr group (Fig. 4C, D). Immunohistochemical staining showed that the expression of Runx2, BSP, and Col1α1 increased and that the expression of ALP and OPN decreased in Lenti-*let-7c*-infected xenografts (Fig. 4E).

Furthermore, western blot analysis showed that the expression levels of ALP and OPN were lower in Lenti-*let-7c*-infected hADSC xenografts than in Lenti-scr-infected hADSC xenografts; while the expression of Runx2 was higher in Lenti-*let-7c*-infected hADSC xenografts (Fig. 4F). In addition, analysis of the ultrastructure of xenografts by transmission electron microscopy indicated that osteocytes displayed a more typical and mature status in Lenti-*let-7c*-infected hADSC xenografts and were characterized by cytoplasmic processes surrounded by a matrix (Fig. 4G). Up-regulation of *let-7c* promoted bone formation, which supported the notion that *let-7c* positively regulates osteogenic differentiation and bone formation in vivo. Furthermore, in the ultrastructure of xenografts, osteoclasts were close to the bone matrix of osteocytes (Fig. 4G), indicating that functional bone tissue was remodeled through bone formation by osteoblasts and bone resorption by osteoclasts.

Prediction and confirmation of the direct target of let-7 in regulating osteogenic differentiation of hADSCs

To investigate the molecular mechanisms of *let-7* regulation of differentiation of hADSCs, we used TargetScan and miRBase to predict the *let-7* potential targets for osteogenesis- or adipogenesis-related genes. Among the candidate target genes, we found that HMGA2, PPARGC1A, PPARGC1B, and SMAD2 have *let-7* binding sites in the 3′-UTR (Fig. 5A). As previously reported, HMGA2 has been shown to be a target of *let-7* [19,31,32], but there are no published articles which have experimental data to show that PPARGC1A, PPARGC1B, and SMAD2 are regulated by *let-7*. To test which one can be targeted in the subset of genes, we constructed luciferase reporter vectors that had either a wild-type (wt) 3′-UTR or a 3′-UTR of those genes containing mu sequences in the *let-7* binding site (Fig. 5B and Supplementary Table S3). Interestingly, we found that only the luciferase reporter activity in the wt HMGA2 3′-UTR was inhibited by *let-7* (Fig. 5C); this is consistent with a previous report that *let-7* represses the expression of HMGA2 [19,31,32]. Western blot analysis further confirmed that endogenous protein expression of HMGA2 was effectively suppressed by *let-7* (Fig. 5D).

To further confirm that the effect of *let-7* is directly mediated by HMGA2, we inhibited endogenous HMGA2 expression in hADSCs using a specific siRNA. ALP staining and assays for the expression and activity of ALP and alizarin red staining for mineralization (Fig. 6A–D), qRT-PCR, and western blotting for the expression of osteogenic differentiation lineage-related genes were performed (Fig. 6E, F). The results indicated that down-regulation of endogenous HMGA2 promoted osteogenic differentiation of hADSCs. In contrast, down-regulation of endogenous HMGA2 suppresses adipogenesis of hADSCs as indicated by oil red O staining for lipids (Fig. 6G).

Discussion

Decreased bone formation that occurs with aging, immobility, or osteoporosis is usually accompanied by an increase in bone marrow adipogenesis [35,36]. Adjusting the balance between bone formation and adipogenesis might be a therapeutic option for the prevention or treatment of bone- and fat-associated metabolic diseases. Several miRNAs involved in regulating osteogenic or adipogenic differentiation of MSCs have been identified, such as miR-204, miR-17-5p, and miR-106a, that were indicated to suppress osteoblast differentiation while promoting adipocyte differentiation [23,24]. In contrast, reports of protective miRNAs that can promote osteogenesis and suppress adipogenesis are rare. In this study, we demonstrated a crucial role of *let-7* family miRNAs in modulating osteogenesis and adipogenesis of hADSCs. In our study, we detected the dynamic temporal expression pattern of miRNAs in mouse femurs. We found that the expression of *let-7c* and *let-7d* increased after birth and peaked at 4 weeks before rapidly decreasing after bone maturation. Previous reports demonstrated that bone formation and mineral apposition rates decrease from the fourth week onward in male C57BL/6J mice [34]. Our findings suggest that *let-7* might be a positive regulator of bone development and osteogenesis of MSCs.

To investigate the role of *let-7* in osteogenesis of hMSCs in vitro and bone formation in vivo, we selected hADSCs as a cell model of hMSCs. These cells were chosen due to their convenient isolation and culture and their effective adipogenic and osteogenic differentiation potential under certain

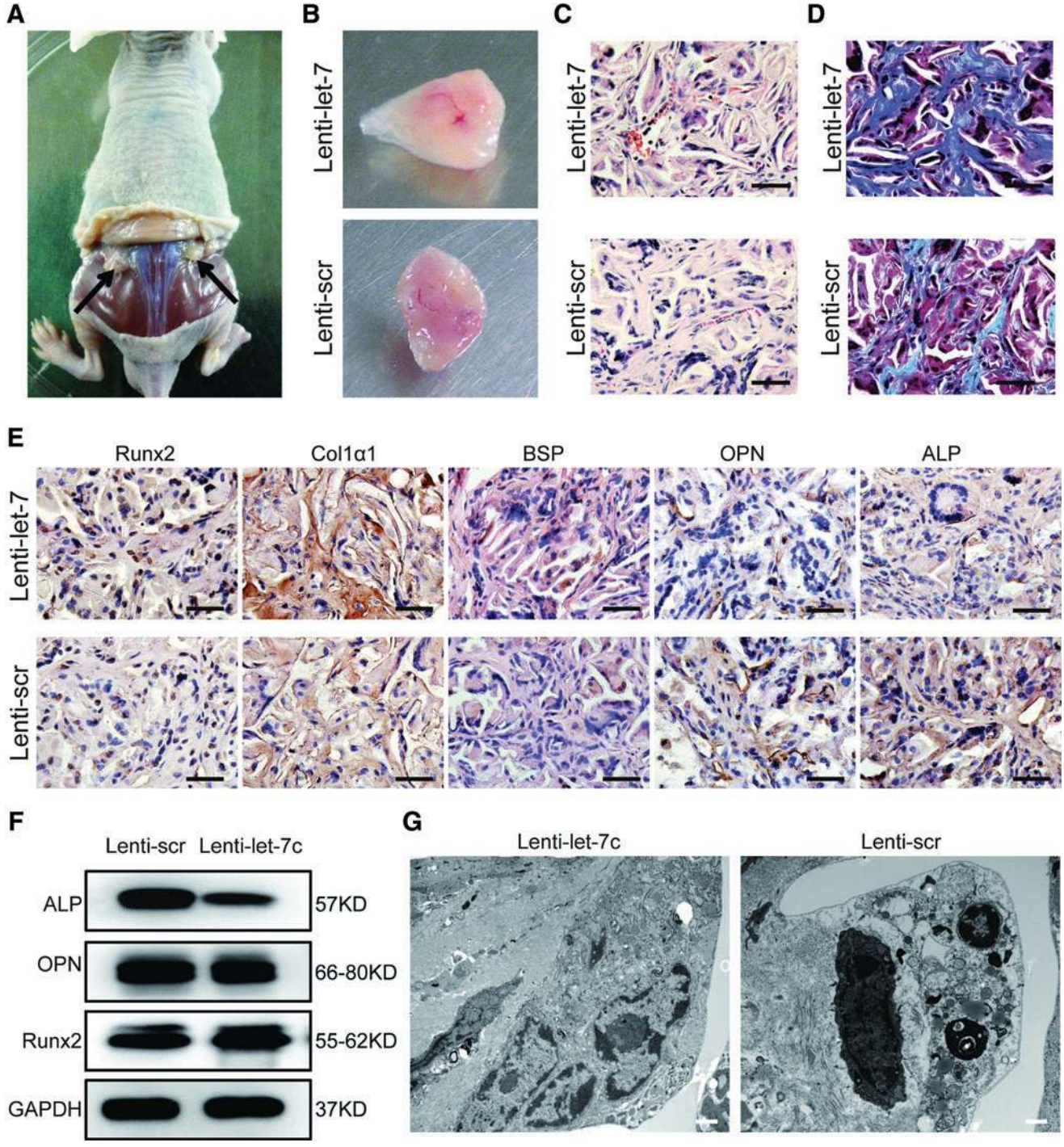

FIG. 4. *let-7* promotes the ectopic bone formation of hADSCs in vivo. The expression of *let-7* was up-regulated by expressing the *let-7c* precursor with a lentiviral vector (Lenti-*let-7c*), and the same lentiviral vector expressing a scrambled sequence (Lenti-scr) was used as a parallel control. **(A, B)** The hADSCs infected with Lenti-*let-7c* and Lenti-scr were loaded on PLGA scaffolds and implanted into 6-week-old male athymic mice (BALB/c nu/nu strain) for 60 days. *Black arrows* indicate xenografts (12 mice/group). **(C)** Hematoxylin and eosin staining of xenografts. Scale bars: 50 μm. **(D)** Masson's trichrome staining analyzed the osteoid formation in xenografts. Scale bars: 50 μm. **(E)** Immunohistochemical staining showed the expression levels of Runx2, bone sialoprotein (BSP), type I collagen alpha 1 (Col1α1), ALP, and OPN in xenografts. Scale bars: 50 μm. **(F)** Western blot analysis indicated the expression of ALP, OPN, and Runx2 in xenografts. $n = 3$. **(G)** The ultrastructure of Lenti-*let-7c*-infected xenografts was observed by transmission electron microscopy. Scale bars: 1 μm. Color images available online at www.liebertpub.com/scd

A

Gene	3'UTR Position	Target site
HMGA2	21-28	5' ...GCCAACGUUCGAUUUCUACCUCA... 3' ... UUGGUAUGUUGGAUGAUGGAGU...
PPARGC1A	38-44	5' ...CAGAGGGAUGGCGAAUACCUCAU... 3' ...UUGGUAUGUUGGAUGAUGGAGU...
PPARGC1B	32-38	5' ...CGAGGAAUACCUCAA ---- UACCUCAG... 3' ... UUGGUAUGUUGGAUGAUGGAGU...
SMAD2	3772-3778	5' ...ACCCAGUUGGUUUCUCUACCUCU... 3' ...UUGGUAUGUUGGAUGAUGGAGU...

B

Primer	Sequence（5'-3'）
HMGA2-wt Forward	5'CTAGAGGGGCGCCAACGTTCGATTTCTACCTCAGCAGC AGTTGGATCTTTTGAAGGGAGAAGACACTGGC3'
HMGA2-wt Reverse	5'GGCCGCCAGTGTCTTCTCCCTTCAAAAGATCCAACTGC TGCTGAGGTAGAAATCGAACGTTGGCGCCCCT3'
HMGA2-mu Forward	5'CTAGAGGGGCGCCAACGTTCGATTTGCAGCAGTTGGAT CTTTTGAAGGGAGAAGACACTGGC3'
HMGA2-mu Reverse	5'GGCCGCCAGTGTCTTCTCCCTTCAAAAGATCCAACTGC TGCAAATCGAACGTTGGCGCCCCT3'

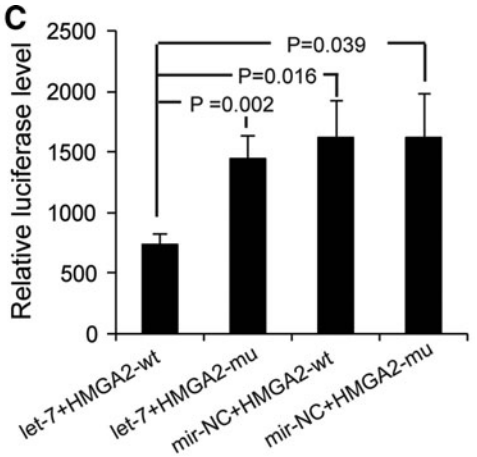

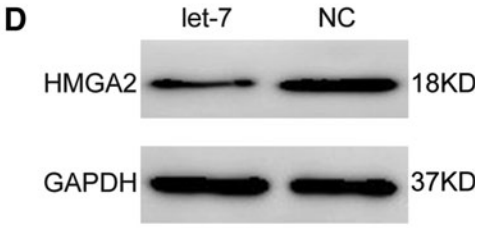

FIG. 5. Prediction and confirmation of the direct target of *let-7* in regulating osteogenic differentiation of hADSCs. **(A)** Bioinformatics analysis showed that target sequences of *let-7* on the 3′-untranslated region (3′-UTR) of its candidate target genes. **(B)** Schematic representation of the luciferase reporter vectors construct containing that had either a wild-type 3′-UTR or a mutant 3′-UTR of high-mobility group AT-hook 2 (HMGA2) coding sequence in the *let-7* binding site. **(C)** *let-7* specifically represses its targets in the luciferase assay in 293T cells. The data are presented as the mean ± SD from three independent experiments. **(D)** Western blot analysis was used to evaluate the expression of HMGA2 when endogenous HMGA2 was inhibited in hADSCs using *let-7*. miR-NC was used as a negative control. $n = 3$.

conditions both in vitro and in vivo [2,3,37,38]. We found that *let-7* overexpression in hADSCs can significantly promote osteogenesis and simultaneously suppress adipogenic differentiation in vitro. When cells were loaded in PLGA scaffolds and implanted into 6-week-old male athymic mice for 60 days, *let-7* upregulation enhanced ectopic bone formation of hADSCs in vivo. We observed the ultrastructure of xenografts using transmission electron microscopy and found that osteocytes generated from hADSCs that overexpressed *let-7* displayed a more typical and mature status which was characterized by cell cytoplasmic processes surrounded by a matrix. Bone tissue is continuously turned over and remodeled through bone formation by osteoblasts of mesenchymal origin and bone resorption by osteoclasts that arise from the hematopoietic lineage [39]. Our results indicated that functional osteocytes and osteoclasts were regulating this dynamic process in bone tissue.

HMGA2 is a member of the high mobility group A family of proteins [40]. It is expressed in almost all tissues at the early developmental stage and then subsequently has limited expression in adults, where it is restricted to tissues of mesenchymal origin [41]. HMGA2 is associated with a variety of common benign mesenchymal tumors and rare aggressive cancers in humans, and it has also been strongly associated with differentiation and development [42,43]. As a non-histone chromatin protein, HMGA2 alters chromatin structure and positively or negatively regulates the expression of many genes [42]. Knockdown of HMGA2 blocks normal cardiac development and completely abrogates in vivo cardiogenesis [44]. HMGA2 also plays a pivotal role in human bone growth and development, and severe mutations in this gene alter body size in both mice and humans [45]. For instance, an 8-year-old boy with severe somatic overgrowth and advanced endochondral bone and dental development had breakpoints at the HMGA2 locus [46]. HMGA2 can be influenced by BMP4, which has been linked to the early steps of adipocyte lineage differentiation of MSCs [47]. These reports suggest that HMGA2 is a negative regulator of bone formation and a positive regulator of adipogenesis.

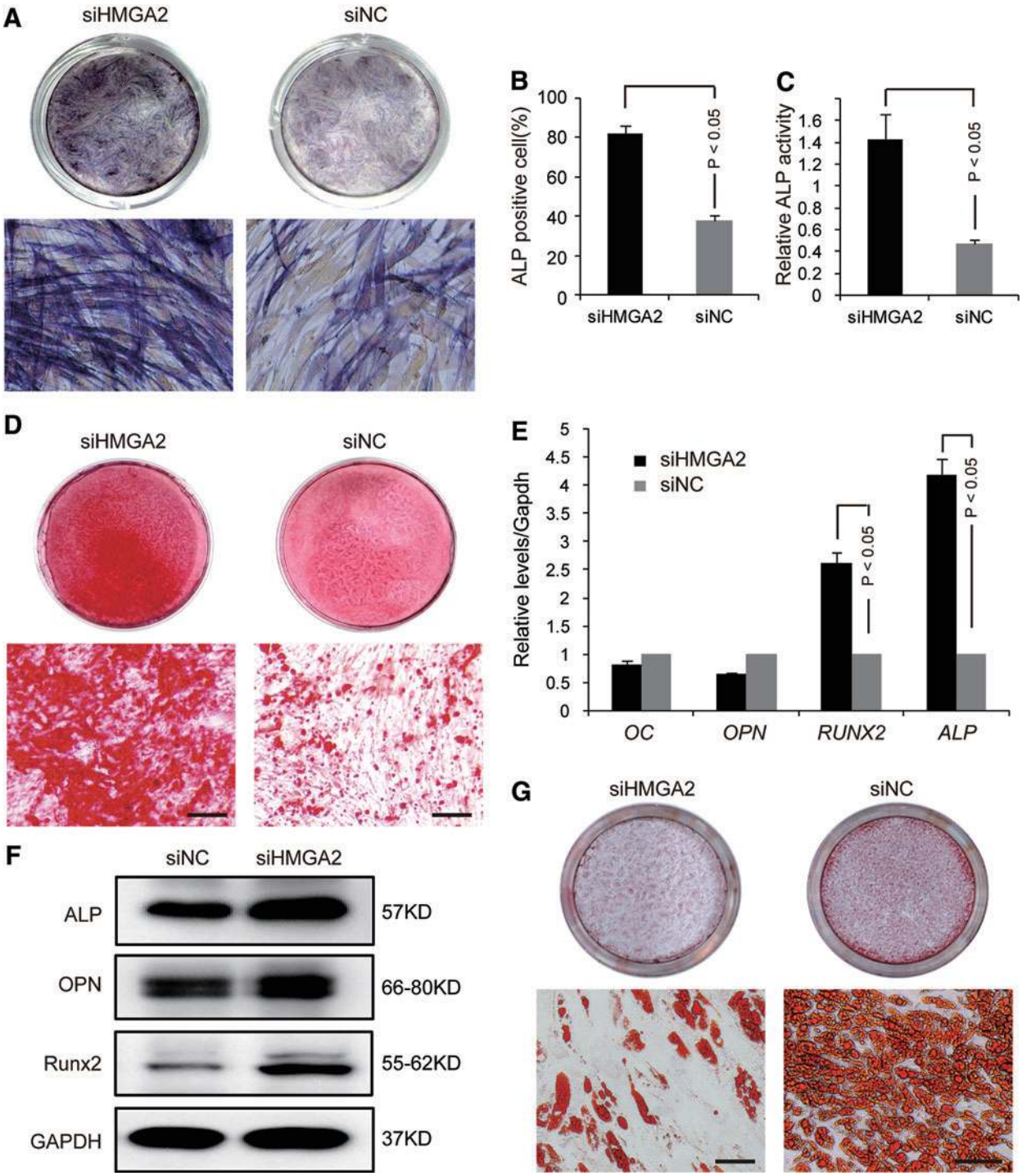

FIG. 6. Down-regulation of HMGA2 promotes osteogenic differentiation and inhibits adipogenic differentiation of hADSCs. **(A)** ALP staining indicated osteogenic differentiation of hADSCs at day 6 when HMGA2 was down-regulated by RNA interference. Scrambled siRNA was used as a negative control. $n = 3$. Scale bars: 100 μm. **(B)** The number of ALP-positive cells was determined by counting under a high power field and normalized by total cell number. The data are presented as the mean ± SD from five independent images of each group. **(C)** ALP activity was calculated during osteogenic differentiation of hADSCs at day 6 when HMGA2 was down-regulated by RNA interference. $n = 3$. **(D)** Alizarin red staining for mineralization indicated the effect of HMGA2 down-regulation on osteogenic differentiation of hADSCs at day 14 by RNA interference. Scrambled siRNA was used as a negative control. $n = 3$. Scale bars: 100 μm. **(E)** qRT-PCR revealed the mRNA expression levels of Runx2, OSX, ALP, and OC during the osteogenic differentiation of HMGA2-inhibited hADSCs at day 6. Scrambled siRNA was used as a negative control. $n = 3$. **(F)** Western blot analysis detected the expression of ALP, OPN, and Runx2 during the osteogenic differentiation of HMGA2-inhibited hADSCs at day 6. Scrambled siRNA was used as a negative control. $n = 3$. **(G)** Down-regulation of HMGA2 affected the adipogenesis of hADSCs as indicated by oil red O staining at day 12. Scrambled siRNA was used as a negative control. $n = 5$. Scale bars: 100 μm. Color images available online at www.liebertpub.com/scd

To investigate the underlying mechanism of *let-7* in balancing osteogenesis and adipogenesis of hMSCs, we identified a set of candidate target genes that contain the binding site of *let-7* in their 3′-UTR and only HMGA2 was confirmed as a target of *let-7*. Several groups also reported that HMGA2 is a *let-7* target gene and that HMGA2 plays a role in regulating adipogenesis and repressing tumorigenesis [19,31,32]. However, how *let-7*/HMGA2 axis regulates osteogenesis is not known until now. Here, we used specific siRNA to downregulate the endogenous expression of HMGA2 and found that osteogenesis was promoted and adipogenesis was suppressed. This was similar to the effect of *let-7* overexpression on the differentiation of hADSCs by targeting HMGA2.

In summary, we showed that *let-7* positively regulates osteogenic differentiation and negatively regulates adipogenic differentiation of hADSCs by repressing HMGA2. Importantly, the temporal expression pattern of *let-7* in mouse femurs is consistent with the timing of bone development. The overexpression of *let-7* can accelerate the osteogenesis of hADSCs and lead to increased bone formation in vivo. Our results suggest that targeting *let-7* expression to promote osteogenesis and suppress adipocyte generation might be used as a novel therapeutic approach for disorders such as osteoporosis that are associated with bone loss and adipocyte accumulation.

Acknowledgments

This work was supported by grants from the ''863 Projects'' of the Ministry of Science and Technology of People's Republic of China (no. 2011AA020100), the National Natural Science Foundation of China (no. 30830052), the National Key Scientific Program of China (no. 2011CB964901), and the Program for Cheung Kong Scholars and the Innovative Research Team in University-PCSIRT (no. IRT0909). The authors thank Xiaoyan Wang for providing them with PLGA scaffold material.

Author Disclosure Statement

All the authors agree that there are no conflicts of interest. No competing financial interests exist.

References

1. Fink T, JG Rasmussen, J Emmersen, L Pilgaard, A Fahlman, S Brunberg, J Josefsson, JM Arnemo, V Zachar, JE Swenson and O Frobert. (2011). Adipose-derived stem cells from the brown bear (*Ursus arctos*) spontaneously undergo chondrogenic and osteogenic differentiation in vitro. Stem Cell Res 7:89–95.
2. Phinney DG and DJ Prockop. (2007). Concise review: mesenchymal stem/multipotent stromal cells: the state of transdifferentiation and modes of tissue repair—current views. Stem Cells 25:2896–2902.
3. Pittenger MF, AM Mackay, SC Beck, RK Jaiswal, R Douglas, JD Mosca, MA Moorman, DW Simonetti, S Craig and DR Marshak. (1999). Multilineage potential of adult human mesenchymal stem cells. Science 284:143–147.
4. Prockop DJ. (1997). Marrow stromal cells as stem cells for nonhematopoietic tissues. Science 276:71–74.
5. Tokuzawa Y, K Yagi, Y Yamashita, Y Nakachi, I Nikaido, H Bono, Y Ninomiya, Y Kanesaki-Yatsuka, M Akita, et al. (2010). Id4, a new candidate gene for senile osteoporosis, acts as a molecular switch promoting osteoblast differentiation. PLoS Genet 6:e1001019.
6. Ambros V. (2004). The functions of animal microRNAs. Nature 431:350–355.
7. Bartel DP. (2004). MicroRNAs: genomics, biogenesis, mechanism, and function. Cell 116:281–297.
8. Ivey KN and D Srivastava. (2010). MicroRNAs as regulators of differentiation and cell fate decisions. Cell Stem Cell 7:36–41.
9. Esau C, X Kang, E Peralta, E Hanson, EG Marcusson, LV Ravichandran, Y Sun, S Koo, RJ Perera, et al. (2004). MicroRNA-143 regulates adipocyte differentiation. J Biol Chem 279:52361–52365.
10. Gerin I, GT Bommer, CS McCoin, KM Sousa, V Krishnan and OA MacDougald. (2010). Roles for miRNA-378/378* in adipocyte gene expression and lipogenesis. Am J Physiol Endocrinol Metab 299:E198–E206.
11. Hu R, W Liu, H Li, L Yang, C Chen, ZY Xia, LJ Guo, H Xie, HD Zhou, XP Wu and XH Luo. (2011). A Runx2/miR-3960/miR-2861 regulatory feedback loop during mouse osteoblast differentiation. J Biol Chem 286:12328–12339.
12. Itoh T, Y Nozawa and Y Akao. (2009). MicroRNA-141 and -200a are involved in bone morphogenetic protein-2-induced mouse pre-osteoblast differentiation by targeting distal-less homeobox 5. J Biol Chem 284:19272–19279.
13. Kim SY, AY Kim, HW Lee, YH Son, GY Lee, JW Lee, YS Lee and JB Kim. (2010). miR-27a is a negative regulator of adipocyte differentiation via suppressing PPARgamma expression. Biochem Biophys Res Commun 392:323–328.
14. Kim YJ, SW Bae, SS Yu, YC Bae and JS Jung. (2009). miR-196a regulates proliferation and osteogenic differentiation in mesenchymal stem cells derived from human adipose tissue. J Bone Miner Res 24:816–825.
15. Li Z, MQ Hassan, M Jafferji, RI Aqeilan, R Garzon, CM Croce, AJ van Wijnen, JL Stein, GS Stein and JB Lian. (2009). Biological functions of miR-29b contribute to positive regulation of osteoblast differentiation. J Biol Chem 284:15676–15684.
16. Li Z, MQ Hassan, S Volinia, AJ van Wijnen, JL Stein, CM Croce, JB Lian and GS Stein. (2008). A microRNA signature for a BMP2-induced osteoblast lineage commitment program. Proc Natl Acad Sci U S A 105:13906–13911.
17. Luzi E, F Marini, SC Sala, I Tognarini, G Galli and ML Brandi. (2008). Osteogenic differentiation of human adipose tissue-derived stem cells is modulated by the miR-26a targeting of the SMAD1 transcription factor. J Bone Miner Res 23:287–295.
18. Mizuno Y, K Yagi, Y Tokuzawa, Y Kanesaki-Yatsuka, T Suda, T Katagiri, T Fukuda, M Maruyama, A Okuda, et al. (2008). miR-125b inhibits osteoblastic differentiation by down-regulation of cell proliferation. Biochem Biophys Res Commun 368:267–272.
19. Sun T, M Fu, AL Bookout, SA Kliewer and DJ Mangelsdorf. (2009). MicroRNA *let-7* regulates 3T3-L1 adipogenesis. Mol Endocrinol 23:925–931.
20. Yang Z, C Bian, H Zhou, S Huang, S Wang, L Liao and RC Zhao. (2011). MicroRNA hsa-miR-138 inhibits adipogenic differentiation of human adipose tissue-derived mesenchymal stem cells through adenovirus EID-1. Stem Cells Dev 20:259–267.
21. Zaragosi LE, B Wdziekonski, KL Brigand, P Villageois, B Mari, R Waldmann, C Dani and P Barbry. (2011). Small

RNA sequencing reveals miR-642a-3p as a novel adipocyte-specific microRNA and miR-30 as a key regulator of human adipogenesis. Genome Biol 12:R64.
22. Zhang J, Q Tu, LF Bonewald, X He, G Stein, J Lian and J Chen. (2011). Effects of miR-335-5p in modulating osteogenic differentiation by specifically downregulating Wnt antagonist DKK1. J Bone Miner Res 26:1953–1963.
23. Huang J, L Zhao, L Xing and D Chen. (2010). MicroRNA-204 regulates Runx2 protein expression and mesenchymal progenitor cell differentiation. Stem Cells 28:357–364.
24. Li H, T Li, S Wang, J Wei, J Fan, J Li, Q Han, L Liao, C Shao and RC Zhao. (2013). miR-17-5p and miR-106a are involved in the balance between osteogenic and adipogenic differentiation of adipose-derived mesenchymal stem cells. Stem Cell Res 10:313–324.
25. Zhang JF, WM Fu, ML He, H Wang, WM Wang, SC Yu, XW Bian, J Zhou, MC Lin, et al. (2011). MiR-637 maintains the balance between adipocytes and osteoblasts by directly targeting Osterix. Mol Biol Cell 22:3955–3961.
26. Roush S and FJ Slack. (2008). The *let-7* family of microRNAs. Trends Cell Biol 18:505–516.
27. Esquela-Kerscher A and FJ Slack. (2006). Oncomirs—microRNAs with a role in cancer. Nat Rev Cancer 6:259–269.
28. Reinhart BJ, FJ Slack, M Basson, AE Pasquinelli, JC Bettinger, AE Rougvie, HR Horvitz and G Ruvkun. (2000). The 21-nucleotide *let-7* RNA regulates developmental timing in *Caenorhabditis elegans*. Nature 403:901–906.
29. Yu F, H Yao, P Zhu, X Zhang, Q Pan, C Gong, Y Huang, X Hu, F Su, J Lieberman and E Song. (2007). *let-7* regulates self renewal and tumorigenicity of breast cancer cells. Cell 131:1109–1123.
30. Goff LA, S Boucher, CL Ricupero, S Fenstermacher, M Swerdel, LG Chase, CC Adams, J Chesnut, U Lakshmipathy and RP Hart. (2008). Differentiating human multipotent mesenchymal stromal cells regulate microRNAs: prediction of microRNA regulation by PDGF during osteogenesis. Exp Hematol 36:1354–1369.
31. Lee YS and A Dutta. (2007). The tumor suppressor microRNA *let-7* represses the HMGA2 oncogene. Genes Dev 21:1025–1030.
32. Mayr C, MT Hemann and DP Bartel. (2007). Disrupting the pairing between *let-7* and Hmga2 enhances oncogenic transformation. Science 315:1576–1579.
33. Cao Y, Z Sun, L Liao, Y Meng, Q Han and RC Zhao. (2005). Human adipose tissue-derived stem cells differentiate into endothelial cells in vitro and improve postnatal neovascularization in vivo. Biochem Biophys Res Commun 332:370–379.
34. Ferguson VL, RA Ayers, TA Bateman and SJ Simske. (2003). Bone development and age-related bone loss in male C57BL/6J mice. Bone 33:387–398.
35. Kajkenova O, B Lecka-Czernik, I Gubrij, SP Hauser, K Takahashi, AM Parfitt, RL Jilka, SC Manolagas and DA Lipschitz. (1997). Increased adipogenesis and myelopoiesis in the bone marrow of SAMP6, a murine model of defective osteoblastogenesis and low turnover osteopenia. J Bone Miner Res 12:1772–1779.
36. Nuttall ME and JM Gimble. (2000). Is there a therapeutic opportunity to either prevent or treat osteopenic disorders by inhibiting marrow adipogenesis? Bone 27:177–184.
37. Kolf CM, E Cho and RS Tuan. (2007). Mesenchymal stromal cells. Biology of adult mesenchymal stem cells: regulation of niche, self-renewal and differentiation. Arthritis Res Ther 9:204.
38. Undale AH, JJ Westendorf, MJ Yaszemski and S Khosla. (2009). Mesenchymal stem cells for bone repair and metabolic bone diseases. Mayo Clin Proc 84:893–902.
39. Lian JB, GS Stein, AJ van Wijnen, JL Stein, MQ Hassan, T Gaur and Y Zhang. (2012). MicroRNA control of bone formation and homeostasis. Nat Rev Endocrinol 8:212–227.
40. Hammond SM and NE Sharpless. (2008). HMGA2, microRNAs, and stem cell aging. Cell 135:1013–1016.
41. Berg JP. (2000). Pygmy mouse gene mutation protects against obesity. Eur J Endocrinol 143:317–318.
42. Fusco A and M Fedele. (2007). Roles of HMGA proteins in cancer. Nat Rev Cancer 7:899–910.
43. Nishino J, I Kim, K Chada and SJ Morrison. (2008). Hmga2 promotes neural stem cell self-renewal in young but not old mice by reducing p16Ink4a and p19Arf Expression. Cell 135:227–239.
44. Monzen K, Y Ito, AT Naito, H Kasai, Y Hiroi, D Hayashi, I Shiojima, T Yamazaki, K Miyazono, et al. (2008). A crucial role of a high mobility group protein HMGA2 in cardiogenesis. Nat Cell Biol 10:567–574.
45. Weedon MN, G Lettre, RM Freathy, CM Lindgren, BF Voight, JR Perry, KS Elliott, R Hackett, C Guiducci, et al. (2007). A common variant of HMGA2 is associated with adult and childhood height in the general population. Nat Genet 39:1245–1250.
46. Ligon AH, SD Moore, MA Parisi, ME Mealiffe, DJ Harris, HL Ferguson, BJ Quade and CC Morton. (2005). Constitutional rearrangement of the architectural factor HMGA2: a novel human phenotype including overgrowth and lipomas. Am J Hum Genet 76:340–348.
47. Markowski DN, BM Helmke, F Meyer, I von Ahsen, R Nimzyk, I Nolte and J Bullerdiek. (2011). BMP4 increases expression of HMGA2 in mesenchymal stem cells. Cytokine 56:811–816.

Address correspondence to:
Dr. Robert Chunhua Zhao
Institute of Basic Medical Sciences
Chinese Academy of Medical Sciences
Center of Excellence in Tissue Engineering
School of Basic Medicine Peking Union Medical College
5# Dongdansantiao
Beijing 100005
China

E-mail: chunhuaz@public.tpt.tj.cn

Received for publication December 10, 2013
Accepted after revision March 6, 2014
Prepublished on Liebert Instant Online March 11, 2014